coatings

MDPI

Article

Effects of Ni/MoS_2, Ag and Cr_2O_3 on the Microstructure and Mechanical Performance of a CoCrFeNi High-Entropy Alloy over a Wide Temperature Range

Chao Xu [1], Dandan Liu [2,*], Chuanwei Zhang [1], Siyu Meng [3] and Bin Wang [2]

[1] School of Mechanical Engineering, Xi'an University of Science and Technology, Xi'an 710054, China; chaoxu@xust.edu.cn (C.X.); zhangcw@xust.edu.cn (C.Z.)
[2] Department of Mechanical and Aerospace Engineering, Brunel University London, Uxbridge UB8 3PH, UK; bin.wang@brunel.ac.uk
[3] School of Water Conservancy and Architectural Engineering, Northwest Agriculture and Forestry University, Xianyang 712100, China; 15129222681@163.com
* Correspondence: 1738009@brunel.ac.uk

Abstract: In the field of aerospace, core components require excellent wear resistance, lubrication and mechanical properties over a wide temperature range. In this study, three groups of CoCrFeNi high-entropy alloy (HEA)-based self-lubricating composites were designed with the addition of Ag, Ni/MoS_2 and Cr_2O_3 using discharge-plasma-sintering technology. Their microstructure, phase composition, mechanical properties, friction and wear properties were analyzed. The results showed that, with the addition of Ag, the hardness and yield stress of HEA-Ni/MoS_2-Ag were reduced by 36 HV and 24 MPa, respectively, while the plastic strain was increased by 2%. With the addition of Cr_2O_3, the hardness (382 HV) and yield stress (430 MPa) of HEA-Ni/MoS_2-Ag-Cr_2O_3 reached their highest values, but the plastic strain reached its lowest value. HEA-Ni/MoS_2-Ag-Cr_2O_3 had the smallest friction coefficient in which the friction coefficient at 800 °C was only 0.42. Additionally, it had a small wear rate of 3.2×10^{-6} mm^3/Nm over a wide temperature range. At lower temperatures, Ni/MoS_2 and Ag were conducive to lubrication, and the wear resistance was improved by the presence of Cr_2O_3. At high temperatures, a nickel oxide phase and a variety of silver molybdate phases were formed via a tribochemical reaction, which was vital to the high-temperature tribological properties.

Keywords: self-lubricating composite; phase composition; microstructure; hardness; compression properties; wide temperature range

Citation: Xu, C.; Liu, D.; Zhang, C.; Meng, S.; Wang, B. Effects of Ni/MoS_2, Ag and Cr_2O_3 on the Microstructure and Mechanical Performance of a CoCrFeNi High-Entropy Alloy over a Wide Temperature Range. *Coatings* **2023**, *13*, 1760. https://doi.org/10.3390/coatings13101760

Academic Editor: Elena Villa

Received: 1 September 2023
Revised: 4 October 2023
Accepted: 9 October 2023
Published: 12 October 2023

1. Introduction

The friction and wear of materials under extremely harsh conditions, especially high temperatures, cause huge economic losses and energy consumption [1,2]. Lubricating materials under wide-temperature-range conditions is vital in this case [3]. The traditional liquid lubrication technology and solid lubrication micro-powder anti-friction coating cannot meet the comprehensive requirements of performance. The use of solid lubrication materials is an effective way to solve friction lubrication under high-temperature conditions [4], which requires a good combination of the lubricating additive phase and the metal matrix and satisfactory mechanical properties.

For the selection of a metal matrix, high-entropy alloys (HEAs) are a new type of material with excellent performance that are used as phase-diagram intermediate solid solutions to break the compositional and structural constraints of traditional alloys [5]. They contain a variety of main elements, which allow the achievement of a low free energy in the system by using a high mixing entropy [6]. At the same time, the formation of complex inter-metallic compound phases is inhibited. A simple and controllable solid solution structure is maintained under the condition of a variety of higher-order principal

components. A large number of lubricating phases is contained in the structure, with multiple principal components and solid solution characteristics, taking into account the excellent mechanical properties and wear resistance [7]. To further improve the wear resistance, multiple materials as lubricants were considered to be added. Wang et al. [8] prepared FeCoCrAl/GNP composites via spark plasma sintering. GNP was present in the form of agglomerated nano-graphite plates and chromium carbide phases. When GPN was not added, the friction coefficient of the alloy was about 0.85 at 5 N, and the wear rate was about 2.5×10^{-4} mm^3/Nm. After adding GPN, graphene was formed in situ on the friction surface, which promoted the formation of nano-abrasive particles and a graphene oxide layer with excellent lubricating properties. In the situation of a frequency of 3 Hz and a load within 30 N, the friction coefficient was lower than 0.15, and the wear rate was lower than 5.67×10^{-6} mm^3/Nm. Xin et al. [9] investigated the various properties of $Al_{0.2}Co_{1.5}CrFeNi_{1.5}Ti_{0.5}$ high-entropy alloys doped with Si. It was found that the hardness of the HEAs was increased due to the addition of Si; at the same time, they exhibited excellent tribological properties. However, the mechanical properties of the alloys, such as compressive strength and fracture toughness, were reduced. Fan et al. [10] studied the influence of an annealing treatment at different temperatures for 24 h on a $CoCrFeNiNb_{0.2}Mo_{0.2}$ high-entropy alloy. It was found that the best mechanical properties were obtained when the annealed temperature was 700 °C.

MoS_2 solid lubricants are some of the most widely used solid lubricants [11]. Yin et al. [12] investigated the friction coefficient and wear rate of flake MoS_2 and bulk MoS_2 when used as coatings. The results showed that the flake MoS_2 had excellent tribological properties because of the low shear strength and the formation of uniform transfer film. MoS_2 maintains a very low coefficient of friction in dry or vacuum environments. However, the friction coefficient gradually increases in high-temperature environments due to its oxidation. Lubrication is therefore reduced or even eliminated [13]. Nevertheless, Li et al. [14] studied the friction and wear properties of nickel-based composites with the addition of different solid lubrication (MoS_2, Ag and V_2O_5). It was found that oxidized MoS_2 and Ag oxides have a tribochemical reaction at high temperatures, generating a good-lubricity silver molybdate phase. In addition, based on previous studies [15], HEA-Ag-Mo composites tribochemically produce Ag_2MoO_4 glaze layers at 800 °C with lubrication and wear reduction. Therefore, Ag is worth considering for their introduction into the composite material. These studies remind us that, while considering lubricity is important, we should also consider the impact of the addition of materials on the mechanical properties.

In this study, a CoCrFeNi high-entropy alloy (HEA) was selected as the matrix, which is one of the representative materials with excellent tensile properties, oxidation resistance and wear resistance, as well as high strength. Its tensile toughness at room temperature is 52%; its tensile fracture strength is 1.1 GPa; and its wear rate is lower than 4×10^{-4} mm^3/Nm from room temperature to 800 °C. At high temperatures, a gradient-dense oxide layer rich in iron in the outer layer, chromium in the middle layer and nickel in the inner layer is formed, resulting in an ideal matrix for new solid lubrication metal materials [16,17]. According to the literature above, two solid lubricants, Ni/MoS_2 and Ag, were added to achieve wide-temperature-range lubrication. The addition of Cr_2O_3 can improve the hardness of the composite material and can further improve the wear resistance [18]. Three kinds of self-lubricating composites, HEA-Ni/MoS_2, HEA-Ni/MOS_2-Ag and HEA-Ni/MOS_2-Ag-Cr_2O_3, were prepared, respectively. The microstructure, morphology and phase composition of the composites were analyzed via SEM, EDS, XRD and Raman spectroscopy, and the tribological properties in a wide temperature range (25 °C, 200 °C, 400 °C, 600 °C and 800 °C) were tested, revealing the friction and wear mechanism of the composites at different temperatures. The research results not only provide a reference and guidance for solving the problem of wide-temperature-range lubrication and the mechanical property conflict of friction pair materials involved in aerospace applications, but they also open up a new method for the development of new and advanced wide-temperature-

range high-entropy-alloy-based self-lubricating composites (see Supplementary Materials for the highlights).

2. Materials and Methods

Ni/MoS_2 was composed of 24 wt.% MoS_2 and 76 wt.% Ni, with less than 0.5 wt.% of impurities. The reaction between MoS_2 and HEA matrix powder was effectively inhibited via Ni coating. The decomposition of solid lubricant during the sintering process was prevented; at the same time, the bonding strength between MoS_2 and HEA matrix powder was improved [16]. Therefore, the process parameters of discharge-plasma-sintering preparation were adjusted as follows: (1) the heating rate from room temperature to 1250 °C was 150 °C/min; (2) 1150 °C lasted for 3 min; and (3) cooling was performed with the furnace. The configurations of the three composite materials are shown in Table 1.

Table 1. Ratio of three composite materials (wt.%).

Sample	Ag	Ni/MoS_2	Cr_2O_3	Others
HEA-Ni/MoS_2	0	15	0	85
HEA-Ni/MoS_2-Ag	12.5	15	0	72.5
HEA-Ni/MoS_2-Ag-Cr_2O_3	12.5	15	5	67.5

The phase composition was detected with an X-ray diffractometer (XRD, D/MAX-2400) at a test voltage of 40 kV and a scanning rate of 2 °C/min. The microstructure and chemical composition of the samples were studied via SEM (JSM-7610F, JEOL, Tokyo, Japan) and EDS (Thermo Scientific UItraDry, Waltham, MA, USA).

The hardness was measured with an HV-1000 Vickers hardness tester at a load of 300 g and a holding time of 10 s. The compression properties were tested on a CMT5202 material testing instrument with dimensions and a rate of Φ 4 mm × 8 mm and 1 mm/min, respectively. The frictional properties were evaluated at room temperature, 400 °C and 800 °C in atmospheric conditions using a ball-on-disc high-temperature tribometer (HT-1000, China). The disc was composed of CoCrFeNi, CoCrFeNi-Ag and CoCrFeNi-Ag-Mo composite materials, and its size was Φ30 mm × 5 mm. The coupling ball was made of Al_2O_3 (2400 HV, Ra ≤ 0.03 μm) with a diameter of Φ6 mm. The friction and wear tests were carried out under the conditions of a load of 8 N, a rotation radius of 4 mm, a sliding speed of 0.15 m/s and a sliding distance of 270 m. The worn and unworn surfaces were studied via scanning electron microscopy (SEM) and energy-dispersive spectroscopy (EDS). The coefficient of friction (COF) was automatically recorded with a high-temperature tribometer. The wear rate (WR, w, mm^3/Nm) was calculated using the formula w = V/FS, where V, S and F are the wear amount (mm^3), the total sliding distance (m) and the normal load (N), respectively. The wear amount (V) was obtained with a non-contact surface profiler (Micro-XAM-3D, Germany). The oxide composition on the worn surface of CoCrFeNi-Ag-Mo alloy at 800 °C was further determined via laser Raman spectroscopy (Thermo, Waltham, MA, USA).

3. Results and Discussion

3.1. Phase Composition

In order to analyze the phase composition of the Ni/MoS_2, Ag and Cr_2O_3 composites, XRD was performed for phase detection and characterization. Figure 1 shows the XRD patterns of the three prepared HEA matrix composites. The face-centered cubic (FCC) phase, Ag phase, Ni phase, MoS_2 phase and Cr_2O_3 phase of the HEA matrix can be obviously observed in the XRD pattern, and no other impurity phase can be seen. For HEA-Ni/MoS_2, the proportions of the phases were 87.8% for the FCC and 12.2% for Ni/MoS_2. For HEA-Ni/MoS_2-Ag, the proportions of the phases were 75.2% for the FCC, 13% for Ni/MoS_2 and 11.8% for Ag. For HEA-Ni/MOS_2-Ag-Cr_2O_3, the proportions of the phases were 63% for the FCC, 12.5% for Ni/MoS_2, 10.5% for Ag and 14% for Cr_2O_3. The existence of the

Ag diffraction peak proves that the Ag phase was precipitated from the HEA matrix. The precipitation of the Ag phase was mainly attributed to the positive enthalpy that occurred when mixing Ag with the Co, Cr, Fe and Ni matrix elements [19]. The rapid discharge-plasma-sintering process and the presence of the Ni coating played a key role in reducing decomposition and reaction during the sintering of the MoS_2 solid lubricant.

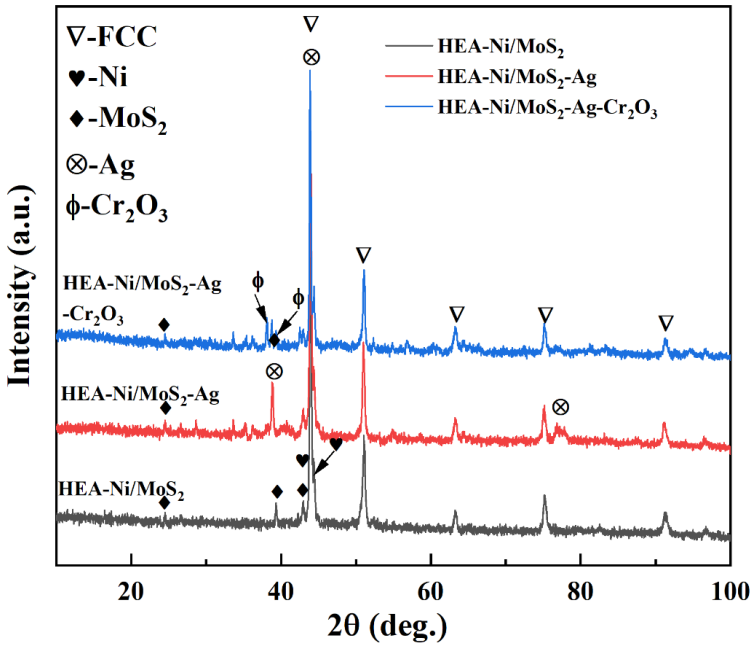

Figure 1. XRD patterns of HEA-Ni/MoS_2, HEA-Ni/MOS_2-Ag and HEA-Ni/MOS_2-Ag-Cr_2O_3.

3.2. Microstructure

As shown in Figure 2, very few pores or other defects appeared in the microstructure of the three composites, indicating that the composites prepared via discharge plasma sintering were close to complete densification. Combined with the EDS data in Table 2, it was determined that Ni/MoS_2 (the B region), Ag (the C region) and Cr_2O_3 (the D region) were distributed at the boundary of the HEA matrix (the A region). The HEA matrix powders were connected with each other via the addition of phase bonding, and the interconnected HEA powders formed a self-lubricating composite matrix. Ni coating effectively inhibited the reaction between MoS_2 and the HEA matrix and improved the bonding strength between the solid lubricant MoS_2 and the HEA matrix. Therefore, the composite may have excellent mechanical and tribological properties over a wide temperature range.

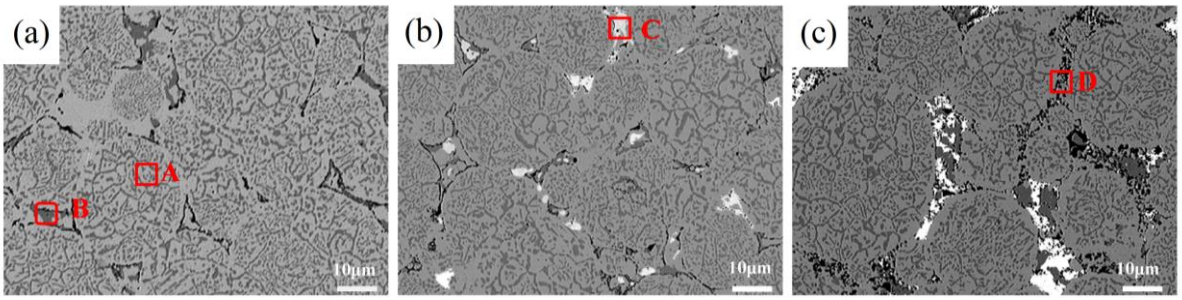

Figure 2. Microstructure of composites: (**a**) HEA-Ni/MoS_2, (**b**) HEA-Ni/MOS_2-Ag and (**c**) HEA-Ni/MOS_2-Ag-Cr_2O_3.

Table 2. EDS statistics of different regions of composites (wt.%).

Area	Co	Cr	Fe	Ni	Mo	S	Ag	O
A	26.14	23.06	24.77	26.03	0	0	0	0
B	0	0	0	72.01	15.92	12.07	0	0
C	0	0	0	0	0	0	100	0
D	0	68.42	0	0	0	0	0	31.58

3.3. Mechanical Property Analysis of Composites at Room Temperature

Figure 3 and Table 3 show the mechanical properties of the composite materials. It can be seen that, due to the addition of the metal Ag, the hardness of HEA-Ni/MoS_2-Ag decreased from 358 HV to 342 HV. In addition, the yield strength decreased from 395 MPa to 371 MPa, while the plastic strain increased from 23% to 25%. The hardness and yield strength of the material decreased with the addition of soft Ag, while the toughness increased [20]. With the addition of Cr_2O_3, the HEA-Ni/MoS_2-Ag-Cr_2O_3 composite expressed the highest hardness (382 HV) and yield strength (430 MPa) values. However, its plastic strain was reduced to the lowest value of 20%. These changes in mechanical properties are attributed to the several additives, which lead to the formation of new phases and changes in HEA grain size [21,22]. The main reason for the strengthening of the HEA-Ni/MoS_2-Ag-Cr_2O_3 alloy was the addition of Cr_2O_3. It was easy to cause stress concentration or cracking during the compression process, which was the reason for the reduction in the toughness of HEA-Ni/MoS_2-Ag-Cr_2O_3.

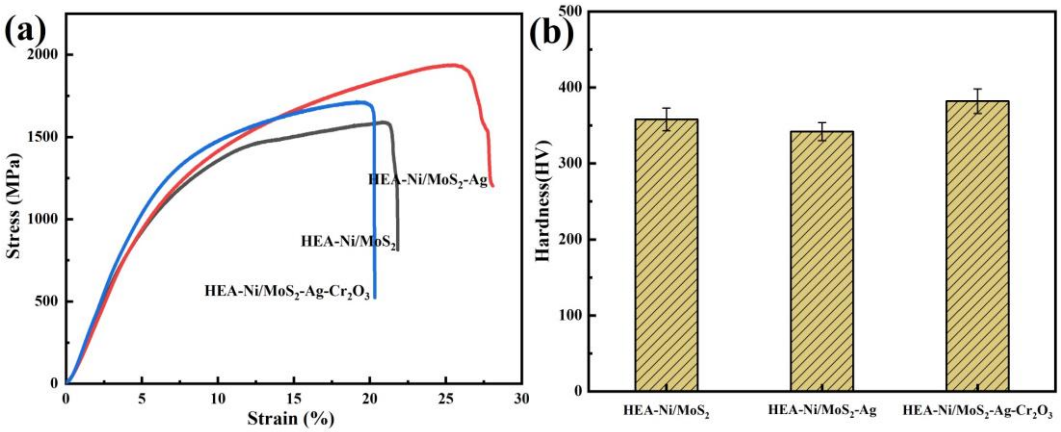

Figure 3. Mechanical properties of the composite: (**a**) compressive stress–strain curve and (**b**) dimensional hardness.

Table 3. Mechanical properties of the composite materials.

Materials	Hardness (HV)	Yield Stress (MPa)	Plastic Strain (%)
HEA-Ni/MoS_2	358	395	23
HEA-Ni/MoS_2-Ag	342	371	25
HEA-Ni/MoS_2-Ag-Cr_2O_3	382	430	20

3.4. Frictional Coefficient

Figure 4a–c depicts the friction coefficient curves of the three composites at the different test temperatures. As shown in Figure 4a, for HEA-Ni/MoS_2, the friction coefficient curve at room temperature was the most stable but had the largest value. As the test temperature increased, the friction curve greatly fluctuated, while the friction coefficient decreased. It can be noted that the friction coefficient significantly decreased, especially at 800 °C. In Figure 4b, the friction coefficient curve of the HEA-Ni/MoS_2-Ag composite material

severely fluctuated. The value of the friction coefficient reached the maximum value at 200 °C, which may have been caused by the generation and accumulation of a large number of wear chips. At the smooth friction and wear stages, the friction coefficients at room temperature and 400 °C were slightly lower than that at 200 °C. The friction coefficients at 600 °C and 800 °C further decreased; nevertheless, the friction curve at 800 °C was the most stable. For the HEA-Ni/MoS_2-Ag-Cr_2O_3 composites (Figure 4c), from room temperature to 400 °C, the friction coefficient of the stationary stage increased with the increase in temperature. The friction coefficients at 600 °C and 800 °C significantly and similarly decreased in value with a stable curve. Figure 4d shows the average friction coefficients of the three composites at the different test temperatures. For HEA-Ni/MoS_2, the highest friction coefficient at room temperature was 0.82. When the temperature rose from 200 °C to 400 °C, the friction coefficient decreased from 0.72 to 0.62. The friction coefficient at 600 °C slightly increased to 0.64. At 800 °C, the friction coefficient significantly decreased, and the lowest value was 0.45. For HEA-Ni/MOS_2-Ag-Cr_2O_3, the coefficient of friction was lower than that of HEA-Ni/MoS_2 from room temperature to 200 °C. Between room temperature to 400 °C, the coefficient of friction was between 0.42 and 0.7. When the temperature rose from 600 °C to 800 °C, the coefficient of friction was about 0.48. The friction coefficient at 600 °C was distinctly lower than that of HEA-Ni/MoS_2. Unlike HEA-Ni/MoS_2 and HEA-Ni/MOS_2-Ag-Cr_2O_3, the friction coefficient of HEA-Ni/MOS_2-Ag at 200 °C was higher than that at room temperature. When the temperature increased from 400 °C to 600 °C, the friction coefficient decreased from 0.61 to 0.42. When the temperature increased from 600 °C to 800 °C, the friction coefficient slightly increased by about 0.44. Over the whole range of experimental temperatures, the friction coefficient was between 0.42 and 0.61. It was obviously lower than those of the other two composite materials, which should be a result of the synergistically good lubricity of Ni/MoS_2 and Ag. The friction coefficients of the three composites remarkably changed with the increase in the test temperature, especially the lower friction coefficient at 800 °C, which was because oxidation played a key role in the tribological properties of the composites [23,24]. In addition, all curves contain some fluctuations along the scratch to some extent, which could be attributed to phase changes and grain orientation [25].

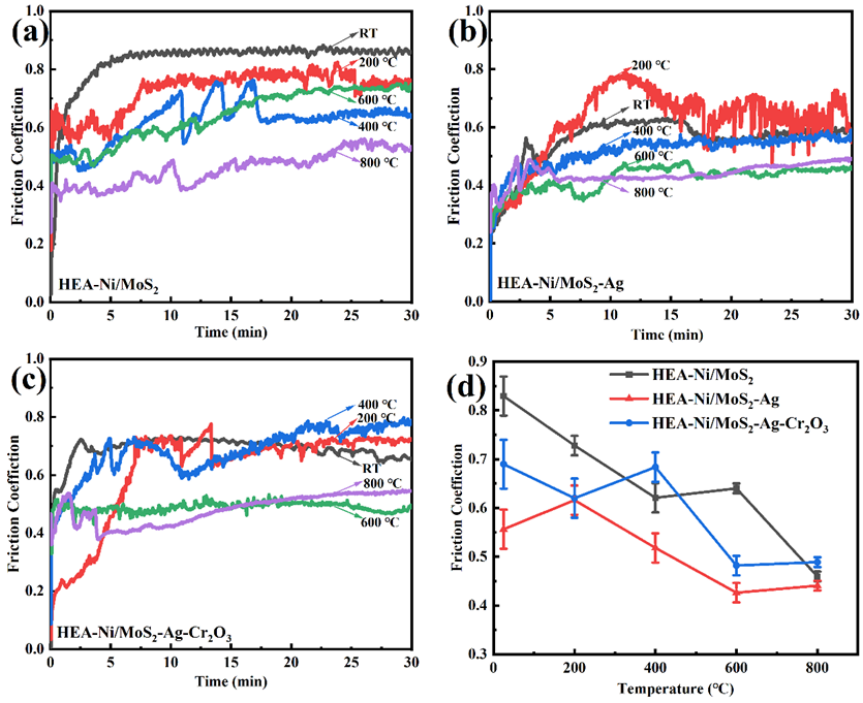

Figure 4. Friction coefficient curves of (**a**) HEA-Ni/MoS_2, (**b**) HEA-Ni/MOS_2-Ag and (**c**) HEA-Ni/MOS_2-Ag-Cr_2O_3 and (**d**) average friction coefficient.

3.5. Wear Rate

In order to better analyze the influence of the progressive addition of Ni/MoS_2, Ag and Cr_2O_3 on the frictional properties of the HEA matrix, a ContourGT-K white light interference 3D profiler was used to characterize the two-dimensional profile of the wear marks. Figure 5a–c shows the two-dimensional profiles of the wear surfaces of the three composites at different test temperatures. It can be seen that none of the curves are smooth because of the accumulation and removal of abrasive chips and the formation of local fractures on the worn surface. The three composites exhibited the deepest and widest wear marks at 200 °C, with depths of 13.3 μm, 13.0 μm and 7.7 μm, respectively, as well as widths of 1.17 mm, 0.78 mm and 1.12 mm. When the temperature increased, the depth or width of the wear marks decreased, reaching the minimum value at 800 °C. The wear rate of the three composites heavily depended on the temperature, which was found by analyzing the change in the height and width of the wear marks. The wear rate reached the maximum value at 200 °C and the minimum value at 800 °C. The average wear rate of the three composites varied with the test temperature, as shown in Figure 5d. From room temperature to 200 °C, the wear rate of the composite material significantly increased with the increase in the temperature and reached the maximum value. With the further increase in the temperature, the wear rate distinctly decreased, and it reached the minimum value at 800 °C. The wear rate of HEA-Ni/MoS_2 at room temperature was about 32.1×10^{-6} mm^3/Nm. It reached the highest value of 139.6×10^{-6} mm^3/Nm at 200 °C and then sharply decreased with the increase in the temperature, and the lowest value, at 800 °C, was 20.5×10^{-6} mm^3/Nm. From room temperature to 800 °C, the wear rate of HEA-Ni/MOS_2-Ag was normally lower than that of HEA-Ni/MoS_2. The wear rate at 200 °C was about 87.4×10^{-6} mm^3/Nm, with a decrease of 37%. The wear rate at 800 °C was about 9.8×10^{-6} mm^3/Nm, with a decrease of 52%. At all the test temperatures, the wear rate of HEA-Ni/MOS_2-Ag-Cr_2O_3 was reduced further than those of the other two composites. Compared with the case of only adding Ni/MoS_2, the wear rate at 200 °C was about 68.1×10^{-6} mm^3/Nm, with a decrease of 51%. The wear rate at 800 °C was about 3.3×10^{-6} mm^3/Nm, with a reduction of 84%. This is consistent with the two-dimensional profile of the abrasion marks in Figure 5a–c. HEA-Ni/MOS_2-Ag-Cr_2O_3 had the best wear resistance over a wide temperature range, mainly due to the co-lubrication of Ni/MoS_2 and Ag, as well as the addition of hard-phase Cr_2O_3, resulting in high hardness [26,27].

It can be seen in the friction and wear experiments that the HEA-Ni/MoS_2-Ag-Cr_2O_3 self-lubricating composite material had the smallest friction coefficient over a wide temperature range, especially the friction coefficient at 800 °C, which was only 0.42. The HEA-Ni/MoS_2-Ag-Cr_2O_3 self-lubricating composite material had a small wear rate of 3.2×10^{-6} mm^3/Nm over a wide temperature range. Under medium- and low-temperature conditions, Ni/MoS_2 and Ag played a lubricating role, and Cr_2O_3 improved the wear resistance. At high temperatures, the phase of NiO and the various silver molybdate phases (Ag_2MoO_4 and $Ag_2Mo_2O_7$) were formed via tribochemical reactions, which had good friction reduction and wear resistance.

3.6. Typical Wear Surface Morphologies

In order to further explore the effect of gradually adding Ni/MoS_2, Ag and Cr_2O_3 to the wear mechanism of the HEA matrix, the friction and wear surfaces of the three composites from room temperature to 800 °C were analyzed. Figure 6 shows the wear surface morphologies of the HEA-Ni/MoS_2 composites at different temperatures. It can be seen in Figure 6 that the wear surface morphology remained good at room temperature. Some tiny furrows and abrasive particles were generated, indicating that the friction process was not very severe, and the main wear mechanism was abrasive wear. When the temperature increased to 200 °C, an obvious furrow morphology, debris accumulation and a few micro-cracks were observed. It can be seen that the main wear mechanisms at this temperature were abrasive wear and slight plastic deformation. This was due to the micro-cutting effect on the composite material during sliding friction resulting from the

high hardness of the dual ball Si_3N_4 (about 1500 HV). When the test temperature was 400, due to abrasive wear, adhesive wear and plastic deformation, a large number of furrows and accumulated wear chips (marked as white areas) were formed on the wear marks. Moreover, with the intensification of oxidation in the high-temperature environment, the formation of an oxide enamel layer on the surface of the wear marks began, which limited the wear resistance. With a further increase in the test temperature, under the combined action of high-temperature oxidation and friction heat, material spalling and accumulation appeared on the wear surface after the friction test at 600 °C. The area that was covered by the oxide enamel layer increased, which played the roles of anti-wear and anti-friction to some extent. This demonstrates that adhesive wear and oxidative wear occurred during the friction process. As the temperature rose to 800 °C, the oxidation behavior was further enhanced. After the friction test, the depth and width of the abrasion marks became obviously narrower. The oxides on the surface of the abrasion marks connected with each other to form a relatively complete black oxide enamel layer and a small number of pits covering the surface of the abrasion marks. The wear mechanism at this temperature was mainly oxidative wear.

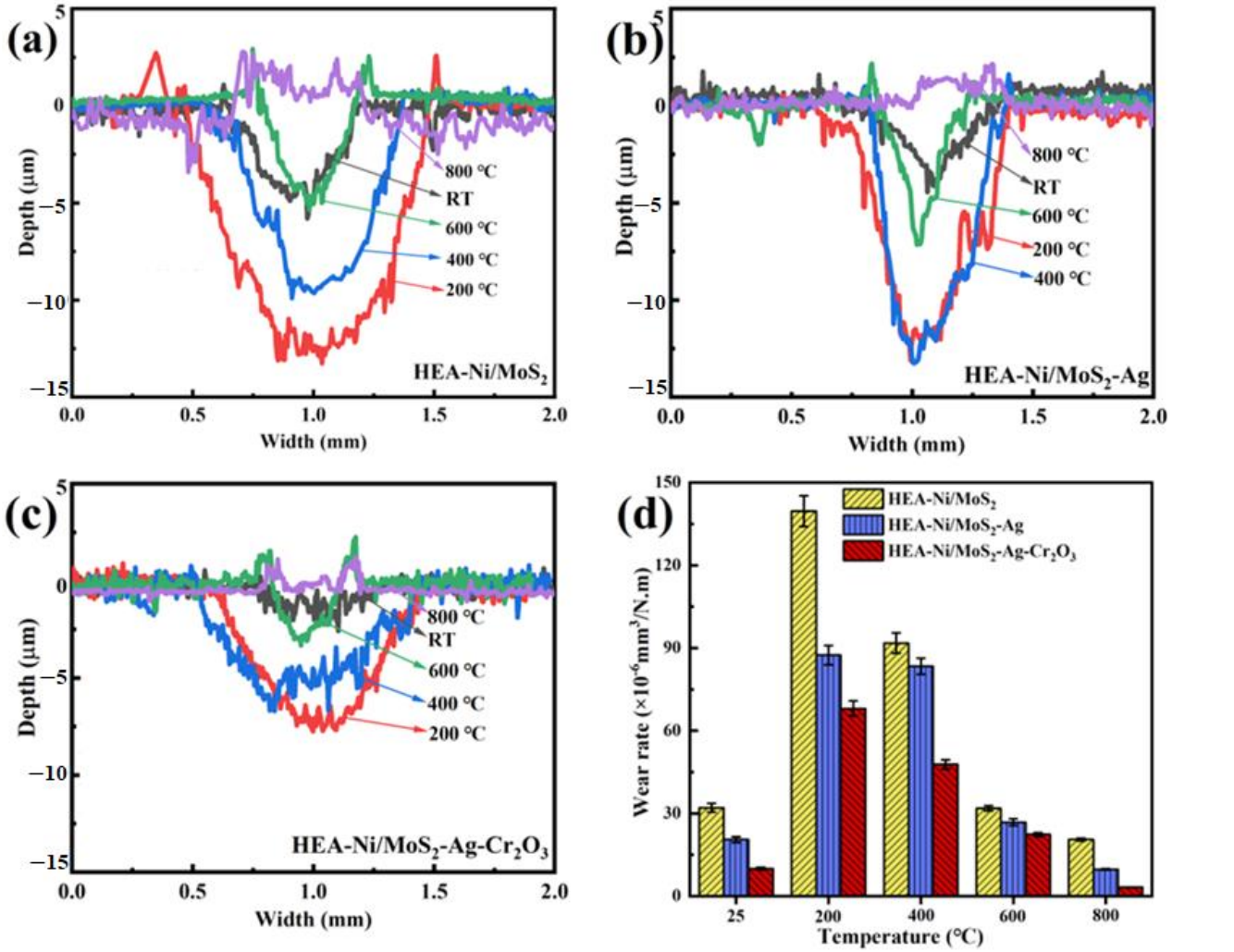

Figure 5. Two-dimensional profile of the wear surface of (**a**) HEA-Ni/MoS_2, (**b**) HEA-Ni/MOS_2-Ag and (**c**) HEA-Ni/MOS_2-Ag-Cr_2O_3 and (**d**) average wear rate.

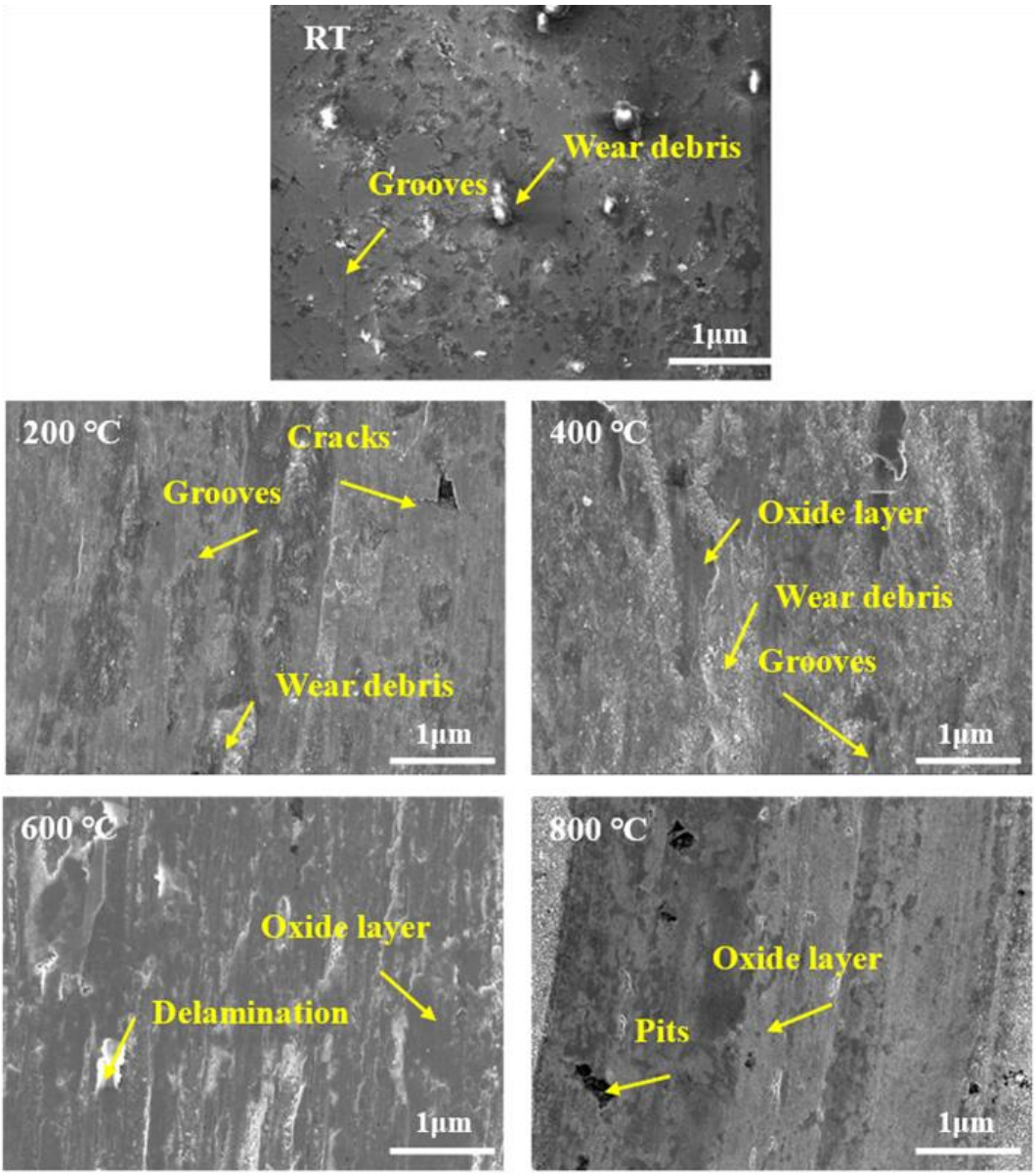

Figure 6. Wear surface morphologies of HEA-Ni/MoS_2 composites at different temperatures.

The wear surface morphologies of the HEA matrix composites containing Ni/MoS_2 and Ag at different temperatures are shown in Figure 7. The addition of the soft Ag phase decreased the strength and hardness of the composite; however, the plasticity and toughness increased. This was conducive to the improvement of the anti-friction properties of the material. At room temperature, the lubrication mechanism of the synergistic addition of Ag and Mo is such that the Ag-rich phase acted as a lubricant, and the Mo-rich phase improved the anti-wear performance [28]. At 200 °C, the abrasive surface became rough, with obvious furrows and more abrasive chips. This was mainly due to the reduction in the strength and hardness of the composite material resulting from the increase in the test temperature and the addition of the soft metal Ag. Therefore, the plowing action of the dual ball was intensified during the friction process, which is in line with the larger fluctuation in the friction coefficient curve at this temperature. At 400 °C, the fine Ag particles formed by diffusion played a role in reducing friction. However, a large number of furrows and abrasive chips and a small number of micro-pits were formed on the wear marks. The matrix and Si_3N_4 spheres adhered to each other with the increase in temperature, resulting in tear pits formed via adhesive wear. At 600 °C, the grooves on

the surface of the wear marks were not obvious, with only some evenly distributed fine debris. Under the interaction of friction heat and friction stress, a soft Ag metal with a large expansion coefficient was constantly extruded from the matrix and oxidized. It may also have tribochemically reacted with Mo oxides to form an incomplete lubrication film with a low shear strength on the wear surface. The main wear mechanisms were abrasive wear and oxidative wear. At 800 °C, the oxidation behavior was further enhanced. The oxidation products on the abraded surface were inter-connected to form a relatively complete, dense and thick black enamel layer and a small number of micro-cracks covering the abraded surface, which could improve the tribological properties of the composite material at 800 °C to a certain extent.

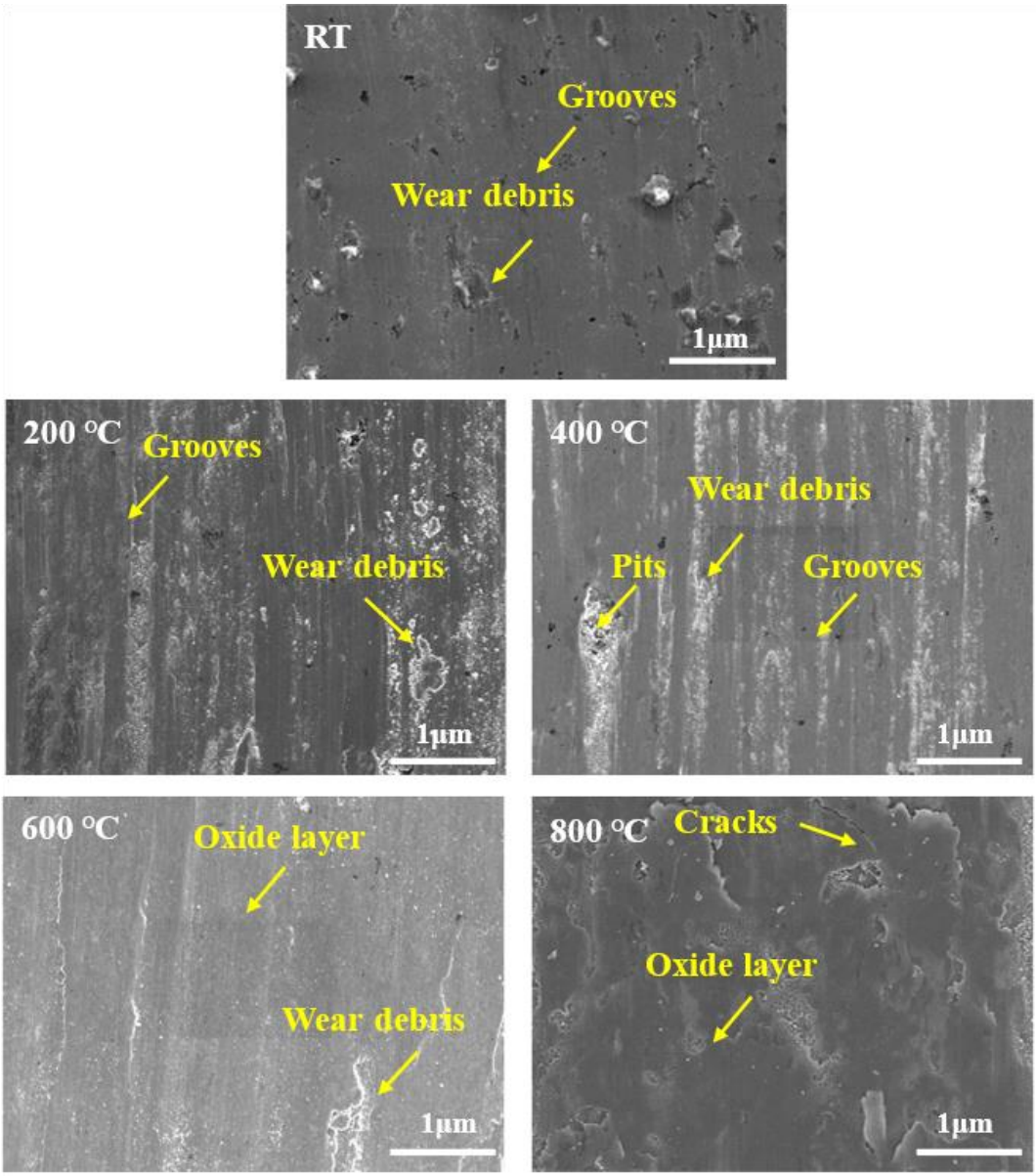

Figure 7. Wear surface morphologies of HEA-Ni/MoS_2-Ag composites at different temperatures.

Figure 8 shows the wear surface morphologies of the HEA-Ni/MoS_2-Ag-Cr_2O_3 composites at different temperatures. It can be seen that the strength and hardness of the composite material increased with the further addition of hard-reinforcement-phase Cr_2O_3, which was conducive to the improvement of the anti-wear performance. At the same time, Ni/MoS_2 and Ag play a lubricating role, and the solid solution strengthening effect of

Mo atoms improves wear resistance [29]. At room temperature, only a small amount of abrasive dust accumulated around the tiny furrows and the HEA-matrix-powder particles. The surface morphology of the material was good, and the wear mechanism was mainly abrasive wear. At 200 °C, the hardness of the composite decreased; simultaneously, there was an obvious furrow morphology as well as wear particles on the surface of the wear marks. The main wear mechanism at this temperature was thus abrasive wear. At 400 °C, the abrasive surface became rough. A large amount of white abrasive chips and a small amount of black oxidation products were formed, indicating that the main wear mechanism was still abrasive wear. Spalling and pitting of the material could be seen on the surface of the wear marks after the friction test at 600 °C. A discontinuous glaze layer was formed by the generated oxides under the synergistic action of normal pressure and friction heat. This glaze layer could improve the tribological properties of the composite in a certain range, indicating that the main wear mechanism was oxidative wear. As the temperature rose to 800 °C, the oxidation behavior was further enhanced. After the friction test, the width of the wear marks significantly narrowed. With the combined action of normal pressure and a higher friction heat, the types and quantities of the oxides generated on the surface of the wear marks increased. A smooth and continuous glazed layer with a certain thickness and high adhesion to the substrate was formed on the wear surface. The direct high-stress contact between the dual ball and the composite material thus transformed into indirect contact between the dual ball and the glaze layer, causing a reduction in the shear stress of the sliding interface. Therefore, HEA-Ni/MoS_2-Ag had excellent tribological properties at 800 °C.

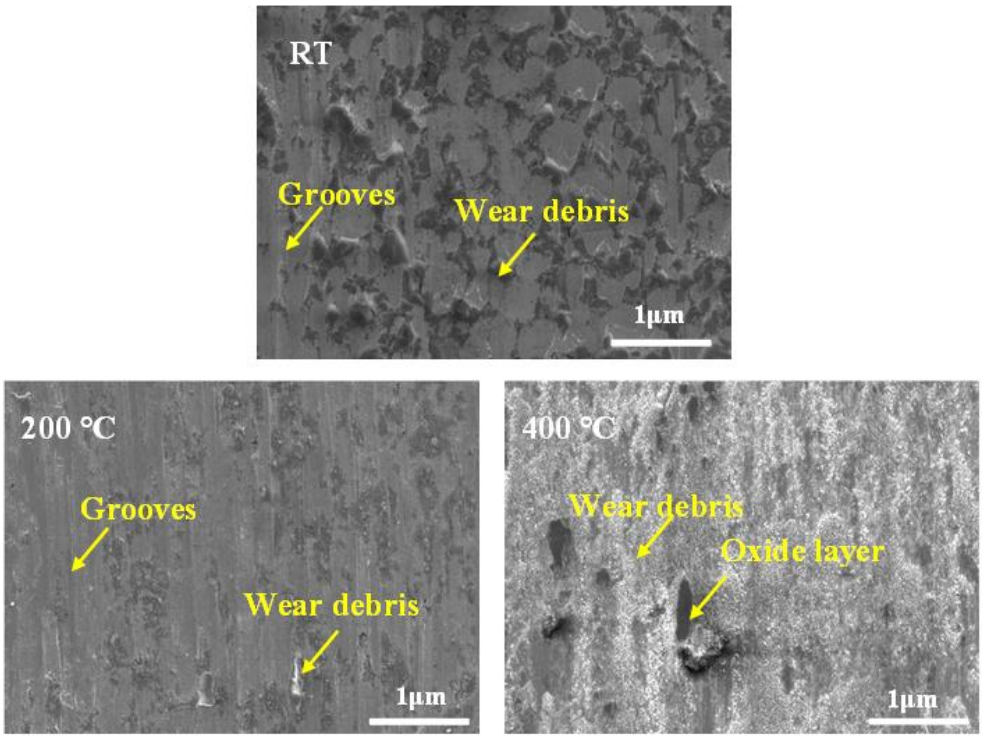

Figure 8. *Cont.*

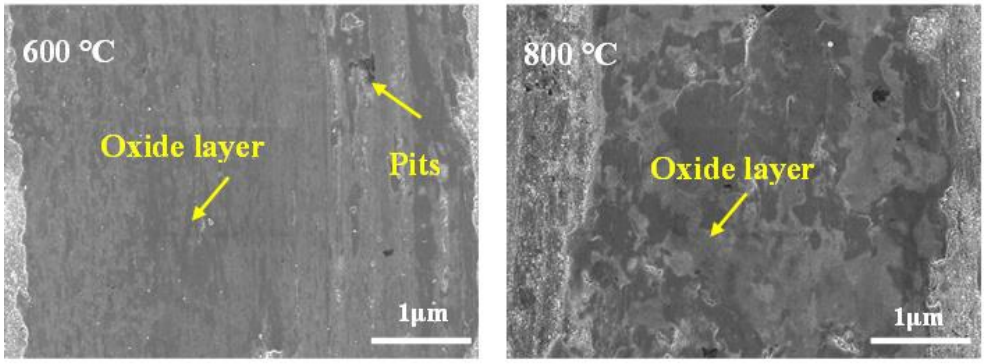

Figure 8. Wear surface morphologies of HEA-Ni/MoS_2-Ag-Cr_2O_3 composites at different temperatures.

It was found that only the HEA-Ni/MoS_2-Ag-Cr_2O_3 composites had both anti-friction and anti-wear tribological properties at 800 °C. The reason for this is the formation of a new phase at a high temperature [30]. Raman spectroscopy was used to characterize the components of the worn surface, as shown in Figure 9. The main component of the oxide was composed of NiO and a variety of silver molybdate (Ag_2MoO_4 and $Ag_2Mo_2O_7$) phases. The highest peak in Figure 9 is around 700 cm^{-1}, which corresponds to the Ag_2MoO_4 phase with the vibration of anti-symmetric stretching [31]. Layered silver molybdate was generated via a tribochemical reaction between Mo oxide and Ag oxide. The weaker Ag-O and O-Ag-O bonds presented in silver molybdate were more likely to be sheared or broken. The synergistic lubrication of the oxide and silver molybdate on the worn surface was the reason the composite material obtained good lubrication at high temperatures [32,33]. At the same time, the smooth oxidized enamel layer on the wear surface prevented direct contact between the matrix and the silicon nitride dual ball, which could improve the wear resistance of the composite.

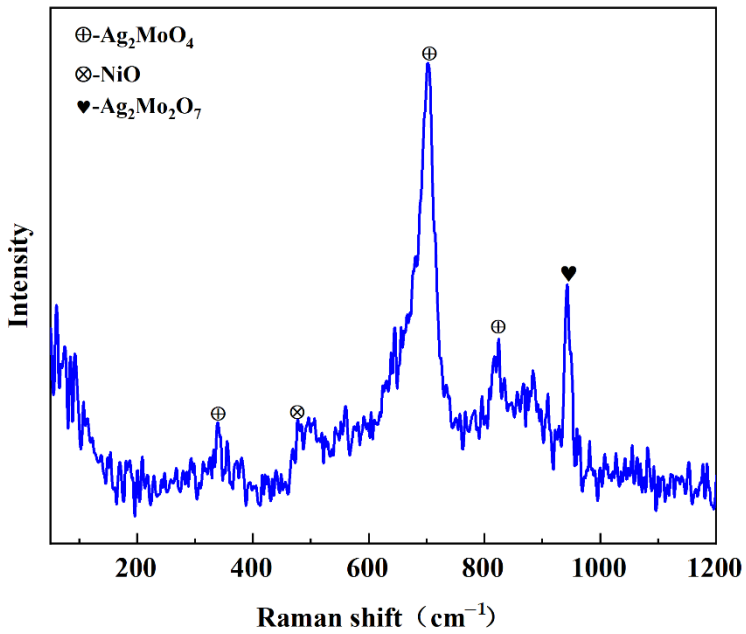

Figure 9. Raman spectra of wear marks of HEA-Ni/MoS_2-Ag-Cr_2O_3 composites after friction test at 800 °C.

4. Conclusions

Three self-lubricating composites, HEA-Ni/MoS_2, HEA-Ni/MOS_2-Ag and HEA-Ni/MOS_2-Ag-Cr_2O_3, were prepared via discharge plasma sintering. The phase com-

position, microstructure, hardness, compression properties and wide-temperature-range tribological properties of the composites were studied. The main conclusions were as follows:

(1) The self-lubricating composite material consisted of the matrix's FCC phase, Ag phase, Ni phase, MoS_2 phase and Cr_2O_3 phase. The added solid lubricant Ni/MoS_2, the soft metal Ag and reinforcement-phase Cr_2O_3 were distributed at the boundary of the HEA matrix.
(2) The addition of Ni/MoS_2, Ag and Cr_2O_3 improved the hardness and yield strength of the material. The HEA-Ni/MoS_2-Ag-Cr_2O_3 self-lubricating composite had the highest hardness value of 382 HV and the highest yield strength value of 430 MPa, while its plastic strain was only 20%.
(3) The HEA-Ni/MoS_2-Ag self-lubricating composite had the smallest friction coefficient over the wide temperature range, especially the friction coefficient at 800 °C, which was only 0.42. The HEA-Ni/MOS_2-Ag-Cr_2O_3 self-lubricating composite had a small wear rate of 3.2×10^{-6} mm^3/Nm over the wide temperature range.
(4) Ni/MoS_2 and Ag played a synergistic role in lubrication. The wear resistance was improved with Cr_2O_3. At high temperatures, NiO and a variety of silver molybdate (Ag_2MoO_4 and $Ag_2Mo_2O_7$) phases were formed via a tribochemical reaction. This enamel layer had good anti-friction and anti-wear properties.

Supplementary Materials: The following supporting information can be downloaded at: https://www.mdpi.com/article/10.3390/coatings13101760/s1.

Author Contributions: Conceptualization, C.X. and D.L.; methodology, C.X.; validation, C.X., D.L. and S.M.; formal analysis, D.L.; investigation, B.W.; resources, C.Z.; writing—original draft preparation, C.X.; writing—review and editing, D.L.; visualization, D.L.; supervision, B.W. and C.Z.; project administration, C.X.; funding acquisition, C.X. All authors have read and agreed to the published version of the manuscript.

Funding: This research was funded by the Key Research and Development Program of Shaanxi Province (Nos. 2022GD-TSLD-63 and 2022GD-TSLD-64).

Institutional Review Board Statement: Not applicable.

Informed Consent Statement: Not applicable.

Data Availability Statement: The data presented in this study are available in this article.

Conflicts of Interest: The authors declare no conflict of interest.

References

1. Luo, J.B.; Liu, M.; Ma, L.R. Origin of friction and the new frictionless technology—Superlubricity: Advancements and future outlook. *Nano Energy* **2021**, *86*, 106092. [CrossRef]
2. Zhai, W.Z.; Bai, L.C.; Zhou, R.H.; Fan, X.L.; Kang, G.Z.; Liu, Y.; Zhou, K. Recent Progress on Wear-Resistant Materials: Designs, Properties, and Applications. *Adv. Sci.* **2021**, *8*, 2003739. [CrossRef] [PubMed]
3. Kumar, R.; Hussainova, I.; Rahmani, R.; Antonov, M. Solid Lubrication at High-Temperatures—A Review. *Materials* **2022**, *15*, 1695. [CrossRef]
4. Gong, H.J.; Yu, C.C.; Zhang, L.; Xie, G.X.; Guo, D.; Luo, J.B. Intelligent lubricating materials: A review. *Compos. Part B Eng.* **2020**, *202*, 108450. [CrossRef]
5. Wang, X.; Guo, W.; Fu, Y.Z. High-entropy alloys: Emerging materials for advanced functional applications. *J. Mater. Chem. A* **2021**, *9*, 663–701. [CrossRef]
6. Chen, J.; Zhou, X.Y.; Wang, W.L.; Liu, B.; Lv, Y.K.; Yang, W.; Xu, D.P.; Liu, Y. A Review on Fundamental of High Entropy Alloys with Promising High–Temperature Properties. *J. Alloys Compd.* **2018**, *760*, 15–30. [CrossRef]
7. Yu, Y.; Qiao, Z.H.; Ren, H.B.; Liu, W.M. Research progress on friction and wear properties of high entropy alloys. *J. Mater. Eng.* **2022**, *50*, 1–17. [CrossRef]
8. Wang, L.; Geng, Y.S.; Tieu, A.K.; Hai, G.J.; Tan, H.; Chen, J.; Cheng, J.; Yang, J. In-situ formed graphene providing lubricity for the FeCoCrNiAl based composite containing graphite nanoplate. *Compos. Part B Eng.* **2021**, *221*, 109032. [CrossRef]
9. Xin, B.B.; Zhang, A.J.; Han, J.S.; Meng, J.H. Improving mechanical properties and tribological performance of $Al_{0.2}Co_{1.5}CrFeNi_{1.5}Ti_{0.5}$ high entropy alloys via doping Si. *J. Alloys Compd.* **2021**, *869*, 159122. [CrossRef]

10. Fan, R.; Zhao, S.C.; Wang, L.P.; Wang, L.; Guo, E.J. Effect of Annealing Temperature on the Microstructure and Mechanical Properties of CoCrFeNiNb0.2Mo0.2 High Entropy Alloy. *Materials* **2023**, *16*, 3987. [CrossRef]
11. Vazirisereshk, M.R.; Martini, A.; Strubbe, D.A.; Baykara, M.Z. Solid Lubrication with MoS_2: A Review. *Lubricants* **2019**, *7*, 57. [CrossRef]
12. Yin, J.N.; Yan, H.; Cai, M.; Song, S.J.; Fan, X.Q.; Zhu, M.H. Bonded flake MoS_2 solid lubricant coating: An effective protection against fretting wear. *J. Ind. Eng. Chem.* **2023**, *117*, 450–460. [CrossRef]
13. Rahman, M.H.; Chowdhury, E.H.; Hong, S. High temperature oxidation of monolayer MoS_2 and its effect on mechanical properties: A ReaxFF molecular dynamics study. *Surf. Interfaces* **2021**, *26*, 101371. [CrossRef]
14. Li, J.; Li, C.S.; Duan, Z.Y. Effect of MoS_2-Ag-V_2O_5 on Friction and Wear Properties of Nickel-based materials. *Powder Metall. Technol.* **2021**, *39*, 141–146.
15. Sun, B. *Preparation and Properties of Cocrfeni High Entropy Alloy Based Self-Lubricating Composites*; Xi'an University of Science and Technology: Xi'an, China, 2023.
16. Sun, Y.; Wu, C.J.; Liu, Y.; Peng, H.P.; Su, X.P. Research status of Influence of alloying Elements on phase composition and mechanical Properties of CoCrFeNi based high-entropy alloys. *Mater. Rev.* **2019**, *33*, 1169–1173.
17. Zhang, A.J.; Han, J.S.; Su, B.; Li, P.D.; Meng, J.H. Microstructure, mechanical properties and tribological performance of CoCrFeNi high entropy alloy matrix self-lubricating composite. *Mater. Des.* **2017**, *114*, 253–263. [CrossRef]
18. Sun, H.W.; Yi, G.W.; Wan, S.H.; Kong, C.L.; Zhu, S.Y.; Bai, L.Y.; Yang, J. Effect of Cr_2O_3 addition on mechanical and tribological properties of atmospheric plasma-sprayed NiAl-Bi2O3 composite coatings. *Surf. Coat. Technol.* **2021**, *427*, 127818. [CrossRef]
19. Geng, Y.S.; Tan, H.; Cheng, J.; Chen, J.; Sun, Q.C.; Zhu, S.Y.; Yang, J. Microstructure, mechanical and vacuum high temperature tribological properties of AlCoCrFeNi high entropy alloy based solid-lubricating composites. *Tribol. Int.* **2020**, *151*, 106444. [CrossRef]
20. Cao, S.L.; Zhou, J.S.; Wang, L.Q.; Yu, Y.J.; Xin, B.B. Microstructure, mechanical and tribological property of multi-components synergistic self-lubricating NiCoCrAl matrix composite. *Tribol. Int.* **2019**, *131*, 508–519. [CrossRef]
21. Daghbouj, N.; Sen, H.S.; Callisti, M.; Vronka, M.; Karlik, M.; Duchon, J.; Čech, J.; Havránek, V.; Polcar, T. Revealing nanoscale strain mechanisms in ion-irradiated multilayers. *Acta Mater.* **2022**, *229*, 117807. [CrossRef]
22. Daghbouj, N.; Sen, H.S.; Č ízek, J.; Lorincík, J.; Karlík, M.; Callisti, M.; Čech, J.; Havránek, V.; Li, B.; Krsjak, V.; et al. Characterizing heavy ions-irradiated Zr/Nb: Structure and mechanical properties. *Mater. Des.* **2022**, *219*, 110732. [CrossRef]
23. Gao, Z.T.; Li, J.Z.; Ke, L.C.; Qiao, Z.H.; Yuan, L.; Gao, Z.M.; Zhang, C.W. Microstructure and tribological properties of in-situ MxB reinforced CoCrFeNi HEA composites prepared by laser cladding. *J. Alloys Compd.* **2023**, *966*, 171560. [CrossRef]
24. Gao, Z.T.; Geng, H.M.; Qiao, Z.H.; Sun, B.; Gao, Z.M.; Zhang, C.W. In situ $TiB_X/Ti_XNi_Y/TiC$ reinforced Ni60 composites by laser cladding and its effect on the tribological properties. *Ceram. Int.* **2023**, *49*, 6409–6418. [CrossRef]
25. AlMotasem, A.T.; Daghbouj, N.; Sen, H.S.; Mirzaei, S.; Callisti, M.; Polcar, T. Influence of HCP/BCC interface orientation on the tribological behavior of Zr/Nb multilayer during nanoscratch: A combined experimental and atomistic study. *Acta Mater.* **2023**, *249*, 118832. [CrossRef]
26. Liu, E.Y.; Gao, Y.M.; Zhang, X.L.; Wang, X.; Yi, G.W.; Jia, J.H. Effect of $Ag_2Mo_2O_7$ incorporation on the tribological characteristics of adaptive Ni-basedcomposite at elevated temperatures. *Tribol. Trans.* **2013**, *56*, 469–479. [CrossRef]
27. Liu, E.Y.; Wang, W.Z.; Gao, Y.M.; Jia, J.H. Tribological properties of adaptive Ni-based composites with addition of lubricious Ag_2MoO_4 at elevated temperatures. *Tribol. Lett.* **2012**, *47*, 21–30. [CrossRef]
28. Kumar, R.; Antonov, M.; Varga, M.; Hussainova, I.; Ripoll, M.R. Synergistic effect of Ag and MoS_2 on high-temperature tribology of self-lubricating NiCrBSi composite coatings by laser metal deposition. *Wear* **2023**, *532–533*, 205114. [CrossRef]
29. Torres, H.; Rojacz, H.; Coga, L.; Kalin, M.; Ripoll, R.M. Local mechanical and frictional properties of Ag/MoS_2-doped self-lubricating Ni-based laser claddings and resulting high temperature vacuum performance. *Mater. Des.* **2020**, *186*, 108296. [CrossRef]
30. Daghbouj, N.; AlMotasem, A.T.; Vesely, J.; Li, B.S.; Sen, H.S.; Karlik, M.; Lorincík, J.; Ge, F.F.; Zhang, L.; Krsjak, V.; et al. Microstructure evolution of iron precipitates in (Fe, He)-irradiated 6H-SiC: A combined TEM and multiscale modeling. *J. Nucl. Mater.* **2023**, *584*, 154543. [CrossRef]
31. Lopes, F.H.P.; Noleto, L.F.G.; Vieira, V.E.M.; Sousa, P.B.; Juca, A.C.S.; Oliveira, Y.L.; Costa, K.R.B.S.; Almeida, M.A.P.; Gouveia, A.F.; Cavalcante, L.S. Experimental and theoretical correlation of modulated architectures of β-Ag_2MoO_4 microcrystals: Effect of different synthesis routes on the morphology, optical, colorimetric, and photocatalytic. *J. Inorg. Organomet. Polym. Mater.* **2022**, *33*, 424–450. [CrossRef]
32. Gulbiński, W.; Suszko, T. Thin films of MoO_3–Ag_2O Binary Oxides—The High Temperature Lubricants. *Wear* **2006**, *261*, 867–873. [CrossRef]
33. Zhang, T.T. *Preparation and Properties of High Temperature Solid Lubrication Coating Materials for Aero Engines*; Institute of Process Engineering, University of Chinese Academy of Sciences: Beijing, China, 2017.